

DIGITAL IMPLEMENTATIONS OF ADAPTIVE FEEDFORWARD AMPLIFIER LINEARIZATION TECHNIQUES

G. Zhao, F. M. Ghannouchi, F. Beauregard and A. B. Kouki

Department of Electrical and Computer Engineering
École Polytechnique de Montréal
C.P. 6079, Succ. Centre Ville
Montréal, Canada H3C 3A7

ABSTRACT

Feedforward power amplifier linearizers using complete digital adaptive control algorithms are proposed. Two different versions, one using frequency domain cancellation and the other using a power gradient approach, are developed. Simulation results, showing carrier signal cancellation in the first loop and distortion cancellation in the second loop for both methods, are presented. This study demonstrates that digital adaptive implementation of feedforward linearization is indeed a promising approach.

INTRODUCTION

Power amplifier linearization plays an important role in communication systems such as PCS. Feedforward linearization, with advantages in bandwidth and generality, is one of three popular approaches (predistortion, feedback and feedforward) that are used for this purpose [1]. The success of this technique depends on its ability to adaptively adjust to changes in temperature or other operation conditions. Although several papers and patents have described different implementations of this technique, none has presented a complete digital adaptive version. In this paper, two digital implementations of feedforward linearizers are proposed. The first implementation employs frequency domain cancellation, while the second one is based on a power gradient algorithm.

DIGITAL ADAPTIVE CONTROL USING FREQUENCY DOMAIN CANCELLATION

Fig.1(a) shows a block diagram of a feedforward amplifier linearizer with a digital adaptive control using frequency domain cancellation. Two pilot signals, f_{p1} and f_{p2} , are introduced to guide the carrier signal cancellation for loop 1, and the distortion cancellation for loop 2, respectively [2].

For loop 1, one of the carriers, f_I , is used as the pilot f_{p1} . In principle, the f_{p1} component at point A should be

zero. In such a case and for an ideal Wilkinson-type inphase combiner, the vector modulator VM1 is adjusted such that the pilot signals at point "a1" and "r1" have equal amplitudes but are 180° out of phase. However, in the present approach, samples of the signals at point "r1" and "a1" are taken by directional couplers and are compared inside the digital controller AC1. Both signals are down-converted with mixers to a low frequency band. The converted signals are then treated by the digital control circuit as shown in Fig.1(b).

The digital band-pass FIR filters reject all but the f_{p1} signals in the two paths. The amplitudes and phases of the two different f_{p1} signals are needed for the adaptive control. Therefore, Fourier transformation is then performed to obtain the two complex amplitudes \mathbf{X} and \mathbf{Y} from two paths. For complete cancellation, \mathbf{X} should be equal to \mathbf{Y} . To compensate for imperfections of the Wilkinson combiner and directional couplers, and any unbalance between the mixers, the signals in both paths are corrected by two calibration factors, \mathbf{C}_r and \mathbf{C}_a , which can be determined by:

$$C_r / C_a = -\alpha_r m_a / \alpha_a m_r \quad (1)$$

where α_r and α_a are the coupling factors of the Wilkinson combiner, \mathbf{m}_r and \mathbf{m}_a represent the factors due to the directional couplers and the mixers.

If \mathbf{X} does not equal to \mathbf{Y} , the vector modulator must be adjusted as follows:

$$\mathbf{K}_n + \mathbf{I} = \mathbf{K}_n (\mathbf{X} / \mathbf{Y})_n \quad (2)$$

where \mathbf{K} represents the complex value of the vector modulator VM1 obtained at point V, n is the index of the segment of the digital data stream with each segment having m iteration samples. The implementation of equation (2) is shown in the block diagram Fig.1(b), where the "Decimator" and "Resample" are necessary for the multirate digital signal processing system.

The adaptive control for loop 2 is similar to that of loop 1, with f_{p1} replaced by f_{p2} . This pilot signal has the same level as the third order intermodulation product, but the frequency differs from all the intermodes. Also, instead of the Wilkinson combiner, a directional coupler with low coupling coefficient must be employed.

The system simulation is done using software SPW (Signal Processing Worksystem) [3] based on complex

WE
2A

envelope concept. A nonlinear model of the main power amplifier is created from its measured AM-AM and AM-PM characteristics. The simulation results reveal that this adaptive control algorithm can quickly track any variation in the amplifier's performance. Even for large deviations, the optimum state can be re-established in few segments. Setting the operation point of the main amplifier at the -3 dB back-off of the 1dB compression, the frequency spectra of the signals at the input, at point A and B, and at the output are shown in Fig.2. In practice, low level parasitic distortions are usually present at the input and are assumed to be at a -80 dBc level. At point A, the cancellation of the first loop yields the third order intermodulation coefficient $IMD_3 = +14$ dBc, meaning that the carrier signal is smaller than the distortion components. The IMD_3 at point B, which indicates the main amplifier's nonlinearity, is -27 dBc, while at the output it is reduced to -80 dBc. It proves that the adaptive control of the second loop works very well. In addition, it is found that for a well-balanced loop 2, the requirement of the residual of the signal cancellation in loop 1 is not as sensitive as that for a non-balanced loop 2. Therefore, a well controlled adaptive loop 2 is important for the whole feedforward linearizer.

DIGITAL ADAPTIVE CONTROL USING POWER GRADIENT IN SERIAL SEGMENTATION

An alternative method is to search for a minimum of the pilot power at point A in loop 1, and at the output in loop 2. For each loop, only one mixer is needed to down-convert the sampled microwave signals, as shown in Fig.3. In the second loop, a filter is necessary to isolate the pilot f_{p2} component, which power is masked by the desired carrier signals from the output. Because it is not difficult to add an FIR filter in the digital signal processing, so that a filter for f_{p1} is still used in loop 1 to improve the minimum power searching.

The algorithm used for finding the minimum of the power is based on the method of steepest descent, expressed as:

$$K(n+1) = K(n) - \alpha \frac{\partial P(n)}{\partial K(n)} \quad (3)$$

where K is the complex value of the vector modulator, α is a gradient coefficient that controls the rate of adaptation and stability, and P is the average power of the pilot signal.

In order to estimate the power gradient in a digital adaptive algorithm, we take every three segments to constitute a long segment in the data stream. As shown in Fig.3(b), let k_r and k_i represent the real and imaginary parts of the complex K , the average power of the pilot is calculated for the three segments in series, with $P_1 = P(k_r, k_i)$, $P_2 = P(k_r + \Delta k, k_i)$, and $P_3 = P(k_r, k_i + \Delta k)$. Then we obtain the following relations:

$$k_r(n+1) = k_r(n) - \frac{\alpha}{\Delta k} [P_2(n) - P_1(n)] \quad (4)$$

and

$$k_i(n+1) = k_i(n) - \frac{\alpha}{\Delta k} [P_3(n) - P_1(n)] \quad (5)$$

where α can be adaptively varied as a function of power level changes, n is the index of the long segment. The adaptive control coefficient K is updated once for each long segment.

This power gradient method only works if the deviation of the main power amplifier's performance is small. Representative simulation results are shown in Fig.4. For the same input $IMD_3 = -80$ dBc, it is found that $IMD_3 = +1.5$ dBc at point A, and $IMD_3 = -42$ dBc at the output, which has about 17 dB improvement comparing with the $IMD_3 = -25$ dBc at the point B. The cancellation levels obtained for both loops are not as good as with the first method using frequency domain cancellation, but are still acceptable for most applications.

CONCLUSION

Two different digital adaptive feedforward linearizers have been studied and simulated. Both are expected to be realized by means of MMIC and DSP chips. Since the principle of the feedforward linearization is to eliminate the intermodulation products in the frequency domain, the first algorithm should be better than the time domain algorithm of the second method, as was confirmed by the presented results. Digital signal processing makes it possible to implement narrow band filters, to perform FFT calculations, and to manipulate data using memory and piecewise operations. Such flexibility is not available in analog implementations. Finally, this study demonstrates that digital adaptive implementation of feedforward linearization is indeed a promising approach.

ACKNOWLEDGMENT

The authors would appreciate Mr. A. Rich for providing the power amplifier's characteristics. The authors also acknowledge the financial support of the Ministère de l'Industrie, du Commerce, de la Science et de la Technologie of Québec, Adventech Inc. and Network Sciences International Ltd. (NSI) as partners in the SYNERGIE program.

REFERENCES

- [1] J. K. Cavers, "Adaptation Behavior of a Feedforward Amplifier Linearizer," IEEE Trans. on Vehicular Technology, Vol. 44, No. 1, Feb. 1995, pp.31-40.
- [2] S. Narahashi and T. Nojima, "Extremely Low-Distortion Multi-Carrier Amplifier ---- Self-Adjusting Feed-Ford (SAFF) Amplifier," in Proc. IEEE Commun. Conf. 1991, pp.1485-1490.
- [3] ALTA GROUP of Cadence Design System, Inc., Signal Processing WorkSystem , 1995.

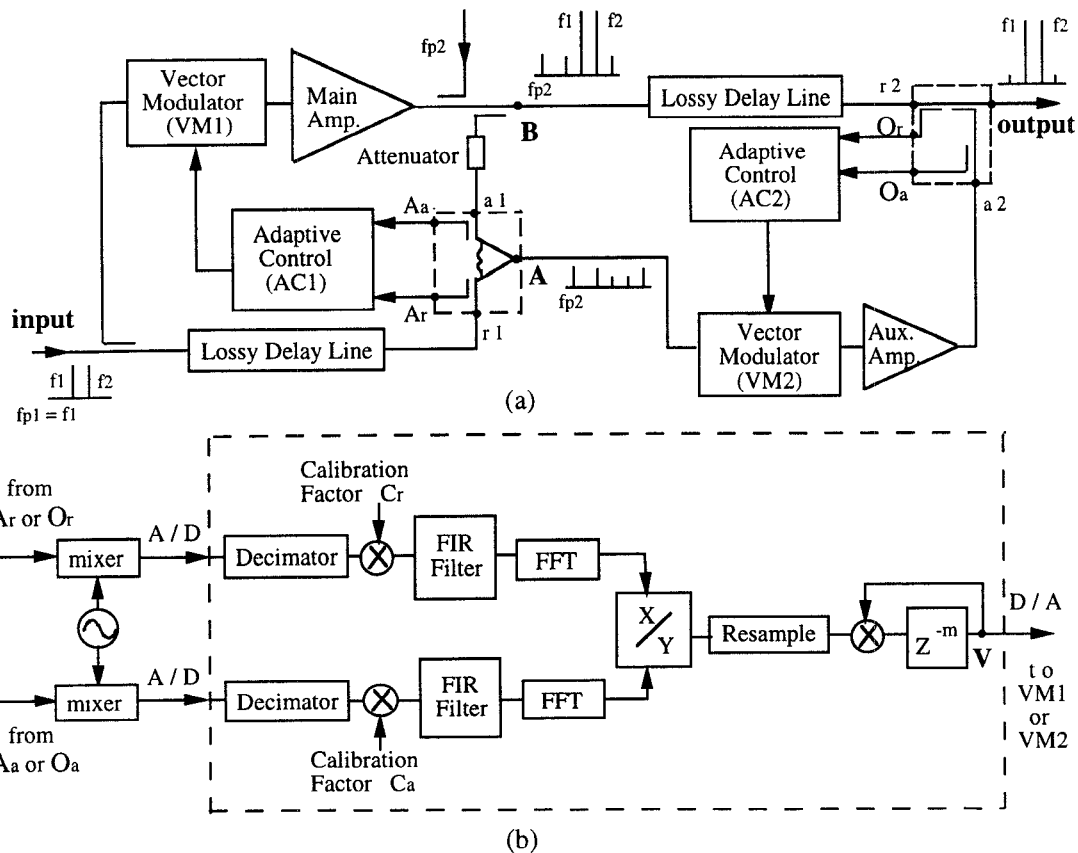


Fig. 1 Block diagram of digital adaptive control using frequency domain cancellation.
 (a) overall system, (b) adaptive controllers.

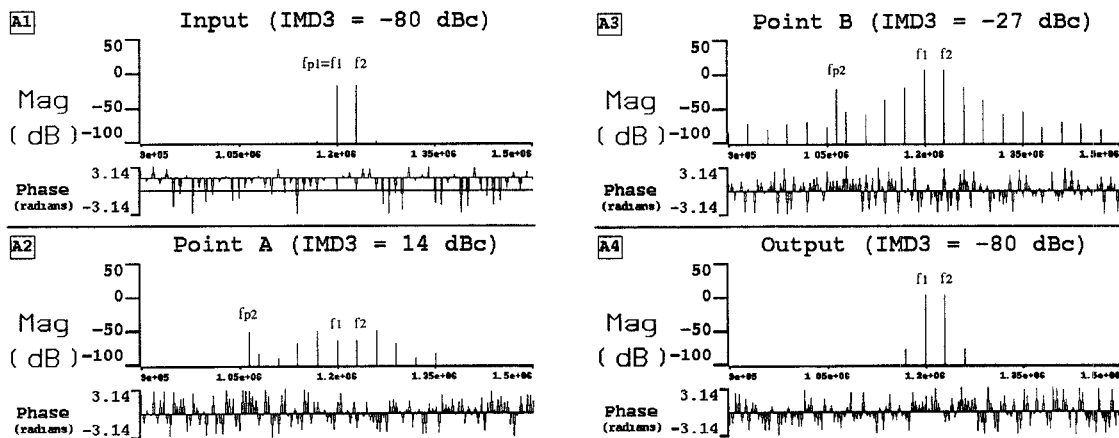


Fig. 2 Frequency spectra of the signals at the input, point A, point B, and at the output (for Fig.1).

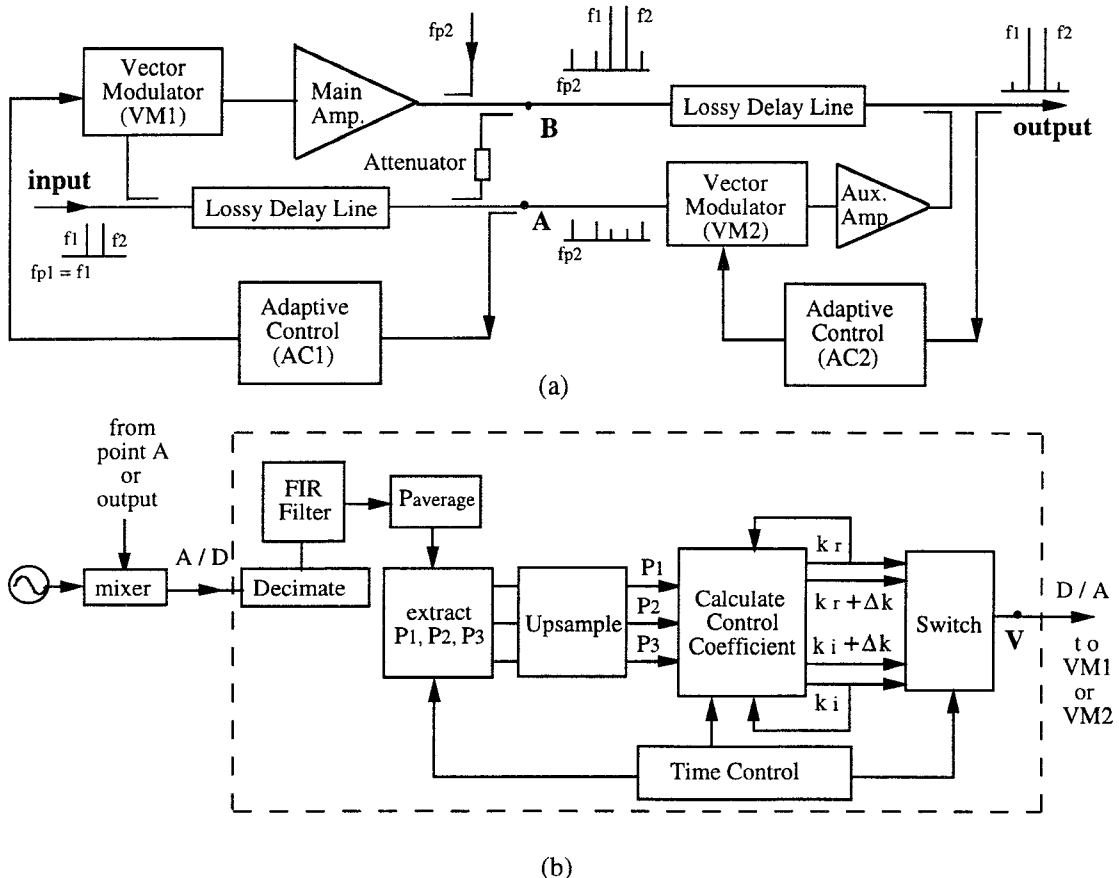


Fig. 3 Block diagram of digital adaptive control using power gradient in serial segmentation.
 (a) overall system, (b) adaptive controllers.

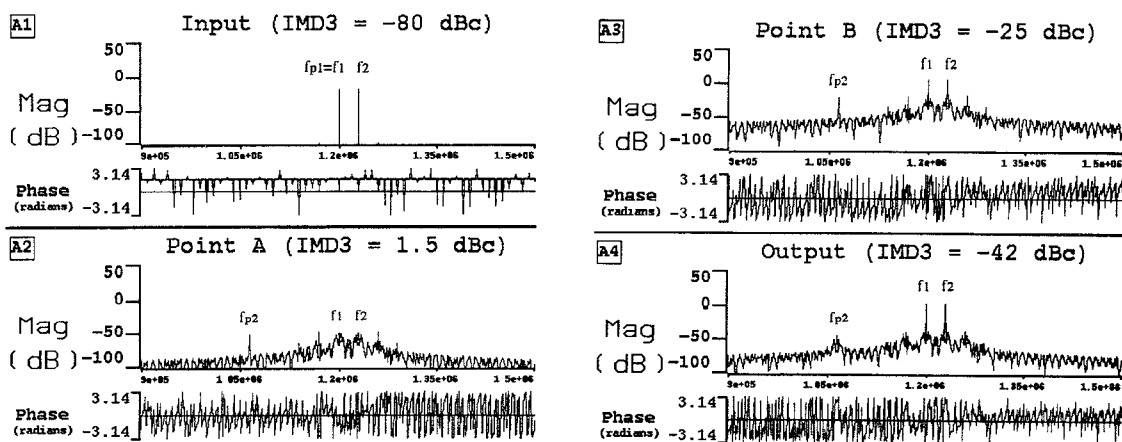


Fig. 4 Frequency spectra of the signals at the input, point A, point B, and at the output (for Fig.3).